

Convalescent Pigs: Liver and Muscle Examination

Ekaterina Vasilevskaya¹, Anastasiya Akhremko, Victoria Pchelkina, and Alexandr Makarenko

V. M. Gorbatov Federal Research Center for Food Systems, Talalikhina st., 26, 109316 Moscow, Russia

Abstract. Comparative studies of muscle tissue and liver of pigs recovered from intracerebral hematoma were carried out using proteomics and histology methods. The absence of pathological changes in the muscles of animals during the accumulation of proteins with molecular weights from 70 to 15 kDa in the muscles of the limbs, from 50 to 20 kDa in the muscles of the back was established. At the same time, destructive changes in the structure of the liver tissue of convalescents were revealed during the accumulation of proteins with masses less than 20 kDa. Thus, it has been shown that in the long-term period after parenchymal hemorrhage in the brain, the consequences of hemorrhagic transformation persist.

1 Introduction

The development of dietary-therapeutic products is one of the most intensively developing areas in the field of applied nutriology [1, 2]. Specialized products are obtained by adding functional compounds, for example, extracts from plant and animal raw materials, to traditional types of products [3, 4]. A sufficient number of functional and specialized products have been developed on the basis of meat. Modern knowledge of the interdependent regulation of the functioning of muscles and the brain indicates the possibility of using in vivo modification to obtain meat with directed properties. The discovered molecular interactions of the muscle-brain axis open the prospect for the use of bioactive protein compounds, actively synthesized in muscles that have lost contact with the central nervous system, to restore the functioning of neuromuscular interactions [5].

The possibility of obtaining meat raw materials for the development of products with neurorehabilitation properties by means of in vivo modification using pigs that have recovered after modeling an intracerebral hematoma has been proven previously [6].

The aim of the work was a comparative study of the muscle tissue and liver of convalescent pigs using proteomics and histology methods to justify the use of by-products.

2 Materials and methods

The objects of the study were muscles *l. dorsi*, *b. femoris*, *m. triceps brachii* and liver of female pigs (n=9): intact, sham-operated and convalescents. Samples were taken from two half-carcasses - left (ipsilateral, corresponding to the brain hemisphere in which the operation was

* Corresponding author: e.vasilevskaya@fncps.ru

performed) and right (contralateral, corresponding to the opposite hemisphere of the brain) - within 20 minutes after slaughter, recovered from intracerebral hematoma (on day 56). Samples for proteomic studies were placed in dry ice; for histological studies, they were fixed in 10% neutral formalin (Biovitrum, Russia) for 7 days at 4°C.

For proteomic studies, a tissue sample (50 mg) was homogenized in 1 ml of buffer containing 7 M urea (Helikon, Russia), 2 M thiourea (Helikon, Russia), 1% wt. dithiothreitol (Helikon, Russia), 0.4% wt. triton X-100 (Helikon, Russia) and 2% vol. ampholines (Serva, Germany), pH 3-10. Homogenizates were centrifuged at a speed of 20,000 g for 20 minutes on a centrifuge (Eppendorf, Germany). One-dimensional electrophoresis was carried out in a 12.5% polyacrylamide gel in the presence of sodium dodecyl sulfate in a chamber (Helicon, USA) at a constant current strength and a voltage of 55 V and 130 V for 2 hours [7]. Protein solutions (Thermo, Latvia) were used as standards. Protein visualization was performed by Coomassie G-250 staining (PanReac, Spain). Band density was determined using the ImageJ program (USA) using 3 gels with equal application. Protein bands on electrophoregrams were interpreted in accordance with databases [8].

For histological studies, tissues after standard alcohol dehydration were embedded in paraffin (Biovitrum, Russia), and sections (10 µm) were obtained on an HM315 microtome (Microm International GmbH, Germany), which were stained with Ehrlich's hematoxylin and 1% eosin aqueous-alcoholic solution (Biovitrum, Russia) according to the methods [9]. The preparations were studied under a light microscope AxioImaiger A1 (Carl Zeiss, Germany). Morphometric studies were carried out using a computer image analysis system AxioVision 4.7.1.0 (Carl Zeiss, Germany). The size of the test zone was 1130×840 µm. At least 100 objects were counted for each section.

To study the ultrastructure, the samples were fixed in a 2.5% solution of glutaraldehyde (PanEco, Russia) followed by additional fixation in a 1% solution of osmic acid in phosphate buffer at pH 7.4 (PanEco, Russia), dehydrated in alcohols of increasing concentration, poured into a mixture of epoxy epon-araldite resin (Biovitrum, Russia). Epoxy blocks were used to make ultrathin sections on an ultratome (Raichart, Holland), which were studied under an electron microscope JEM-100B (Jeol, Japan).

Statistical significance was calculated in the STATISTICA 10 program using Student's t-test, the probability of $p < 0.05$ was chosen as a significant level, the results are presented as "Mean ± Standard Deviation" ($M \pm m$).

3 Results and Discussion

A wide range of protein compounds was found in muscle and liver samples (fig. 1). Major protein bands were identified for the samples of each group of animals (250-150 kDa), probably the extracellular matrix protein tenascin (213.61 kDa), myosin-4 (223.19 kDa), the transmembrane protein tyrosine phosphatase (159.34 kDa), adenylate kinase isoenzyme 1 (29.11 kDa), peroxiredoxin 3 (28.47 kDa), dynactin subunit 6 (20.68 kDa), tubulin alpha chain (52.74 kDa). Liver samples included major structural proteins: unconventional myosin-VI (144.86 kDa); liver carboxylesterase (62.02 kDa); arginase-1 (35.02 kDa); selenoprotein s (21.28 kDa); erythropoietin (21.28 kDa).

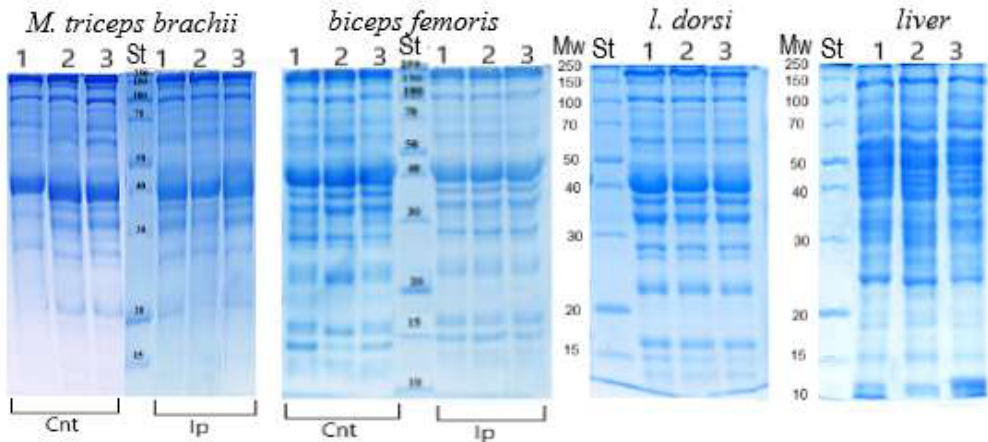


Fig. 1. SDS-PAGE protein profiles of porcine muscles (Cnt – contralateral and Ip – ipsilateral sides) and liver. 1 – intact animals; 2 – sham-operated animals; 3 – convalescent animals. St -standards Mw top down: 250, 150, 100, 70, 50, 40, 30, 20, 15 and 10 kDa.

Grouping the areas of the bands by molecular weight ranges (fig. 2) showed differences between the bands depending on the test matrix in relation to the bands of the samples of intact pigs. For tissues of *m. triceps brachii* and *b. femoris*, on the contralateral side, an increase in protein staining density in the range of 70, 40, 30, and 20 kDa was noted, and on the ipsilateral side, in the range from 40 to 15 kDa. For *l. dorsi*, the accumulation of protein fractions in the range of molecular weights of 50-40, 30 and 20 kDa was revealed. The most significant changes in the intensity of staining of liver proteins were observed in the area of less than 20 kDa, probably glutaredoxin-1 (11.83 kDa), glycoprotein MHC class I SLA-PG6II (12.30 kDa) and liver-expressed antimicrobial peptide 2 (13.13 kDa). The intensity of protein staining increased from sham-operated animals and is most pronounced in convalescent animals.

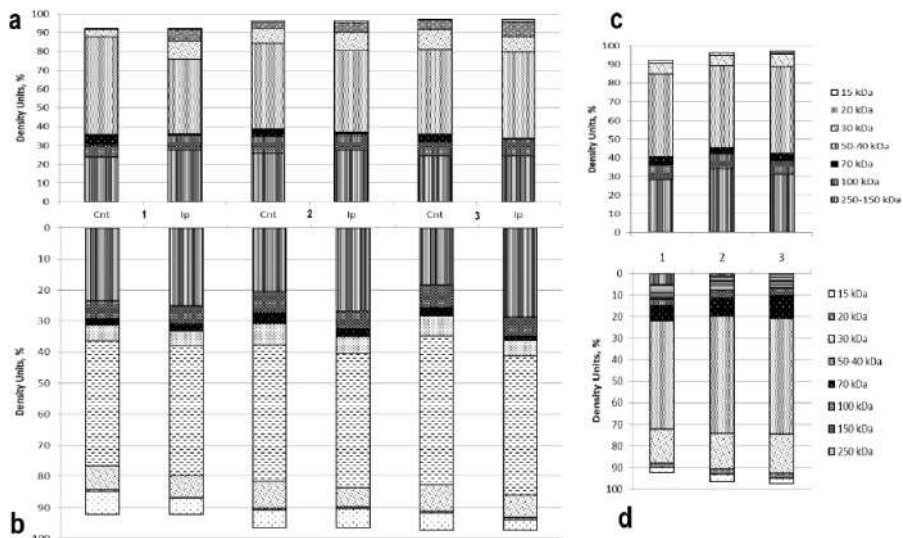


Fig. 2. Molecular weight distribution of porcine muscle and liver proteins. Molecular weight ranges for band regions. a – *m. triceps brachii*; b – *b. femoris*; c – *l. dorsi*; d – liver; 1 – intact animals; 2 – sham-operated animals; 3 – convalescent animals; Cnt – contralateral, Ip – ipsilateral sides.

In a histological study of the muscles of intact and sham-operated pigs on a transverse section, rounded muscle fibers were characterized by dense packing in bundles of the first order. The layers of endomysium are well expressed, in the layers of perimysium there were areas of adipose tissue of a typical structure. Oval-shaped nuclei in muscle fibers were located directly under the sarcolemma. Signs of dystrophic processes, traumatic injuries, hemorrhages were not found. The muscle tissue of the convalescents was characterized by the absence of structural changes. Adipose degeneration, inflammatory or hydropic changes were not noted. Electron microscopy of the muscle tissue of animals of all groups revealed sarcomeres consisting of clearly oriented myofibrils with light and dark discs. Transverse striation without disturbances, signs of destruction of sarcomere elements were not revealed.

The structure of the liver of intact animals is represented by hexagonal acini (Fig. 3, 1A). In the lobules, beams of hepatocytes forming the parenchyma of the organ were clearly defined. The total number of cells was 856.2 ± 12.3 , while the number of dead cells was 140.5 ± 1.6 , the area of hepatocytes was $361.3 \pm 21.2 \mu\text{m}^2$.

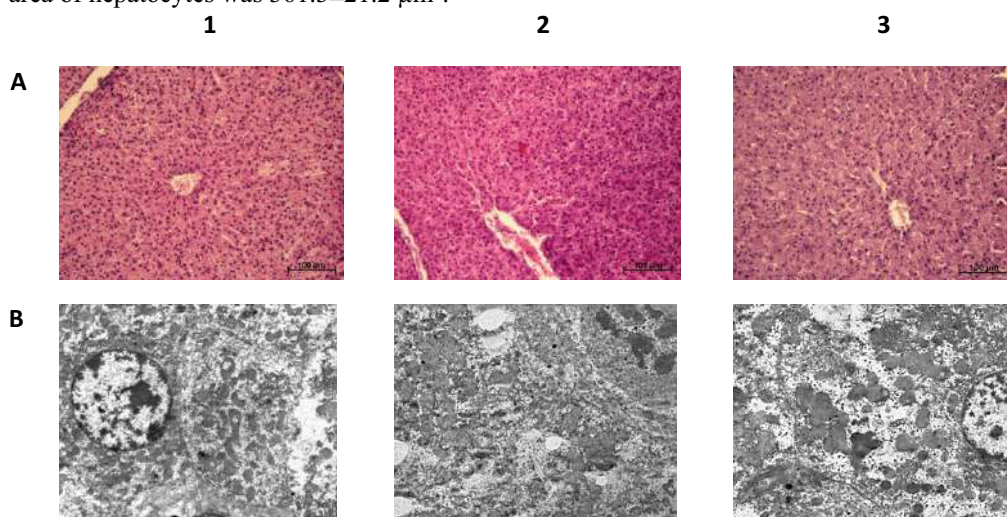


Fig. 3. Pig liver structure. 1 – intact animals; 2 – sham-operated animals; 3 – convalescent animals. A – staining with hematoxylin and eosin (objective 40x, ocular 10x); B – electron microscopy (mag. $\times 8500$).

The nuclei of hepatocytes stained well on the preparation, had a rounded shape and were located in the central part of the cells; the area of the nucleus was $67.3 \pm 2.8 \mu\text{m}^2$. Sinusoidal hemocapillaries were located between the beams. A portal vein was identified at the junctions of several classical lobules. Pathological changes in the acini or hepatocytes, an increase in the lumen of the bile or sinusoidal capillaries were not detected. Hepatocytes had an irregular hexagonal shape with indistinct corners. The elements of the endoplasmic reticulum are well expressed, consisted of dense stacks of tubules and cisterns, located near the nucleus and on the periphery of the cells, in the places of secretion of synthesis products. The cytoplasm of cells is weakly osmiophilic, with a significant amount of mitochondria, free ribosomes, and glycogen granules. There were isolated lysosomes. In some hepatocytes, vacuoles of various shapes and sizes were present in the cytoplasm. The cells were in close contact with each other by dictyosomes. There were no signs of pathological changes in the liver cells, hepatocytes had normal ultrastructural organization (Fig. 3, 1B).

The liver of sham-operated pigs was characterized by some changes in the structural organization of hepatocytes. Pathological disorders of a destructive nature were not established (Fig. 3, 2A). The number of cells was 812.0 ± 7.0 . Hepatocytes were characterized by a decrease in the cell area relative to intact cells to $297.0 \pm 19.0 \mu\text{m}^2$ (by 17.8%, $p < 0.05$), the cytoplasm was

intensely stained, the cell nuclei were unchanged, their area was $65.9 \pm 2.2 \mu\text{m}^2$. The number of dead cells increased relative to the intact cells by 9.7% ($p < 0.05$), amounting to 154.1 ± 2.4 , their cytoplasm was more intensely stained. An increase in the lumen of the sinusoidal ducts was not observed. Electron microscopic analysis revealed an increase in the number of granules with bile secretion and mitochondria, which filled most of the volume of the cell cytoplasm. In the cytoplasm of some cells, loci with hydropic changes were noted. The nuclei of hepatocytes were characterized by a decrease in the density of heterochromatin. Pronounced destructive disorders were not observed, the identified changes indicate the activation of synthetic processes in the liver (Fig. 3, 2B).

Morphology of the liver of convalescents was characterized by significant changes (Fig. 3, 3A). Hepatocytes were in a state of hydropic swelling: nuclear area - $84.6 \pm 3.3 \mu\text{m}^2$, hepatocyte area - $453.3 \pm 27.2 \mu\text{m}^2$, which was 25.7% and 25.5% ($p < 0.05$) more than that of intact cells. The number of hepatocytes per unit area decreased relative to intact cells by 10.2% ($p < 0.05$) and amounted to 769.2 ± 13.8 . In some areas of the acini, a slight infiltration of leukocytes into the sinusoidal ducts was recorded. Hepatocytes, especially in the peripheral areas of the lobules, retained their structure. In some lobules, in their central zones, hepatocytes were found with signs of vacuolization and lysis of the cytoplasm, a large number of cells with pyknotic nuclei. The number of dead hepatocytes was 231.3 ± 3.6 , which was 64.6% more relative to intact cells ($p < 0.05$). Changes in the large blood vessels of the lobules were not found, but changes in the microvasculature were clearly determined: the lumen of the sinusoidal capillaries increased significantly, spaces formed between the beams of hepatocytes. Microcirculatory changes in the liver were mainly diffuse. Electron microscopic examination of hepatocytes revealed differential ultrastructural changes: swelling of the cytoplasm with reduction of organelles; a decrease in the number of secretory granules, mitochondria, ribosomes, elements of the endoplasmic reticulum and glycogen granules, which indicates structural and functional changes in the liver (Fig. 3, 3B).

4 Conclusions

The areas of muscle protein staining in convalescent pigs were increased relative to intact and sham-operated animals. For muscle tissues (*m. triceps brachii*, *b. femoris*), on the contralateral side, an increase in the intensity of protein bands in the region of 35-45 kDa was noted, presumably containing troponin T, fast skeletal muscle (35.35 kDa), malate dehydrogenase (37.70 kDa), creatine kinase (44.60 kDa) and in the 90-110 kDa region (possibly phosphoinositidophospholipase C (106.04 kDa), glutamate receptor (95.45 kDa), actin alpha 2 (101.52 kDa); on the ipsilateral - bands in the range from 15 to 40 kDa, presumably containing MLC1f (20.92 kDa), alpha(B)-crystallin (20.13 kDa), caveolin (17.11 kDa) and creatine kinase (14.87 kDa). Light microscopy and ultrastructural studies of muscle tissue showed the absence of pathological changes in the muscles of animals.

In the long-term period after intracerebral hematoma, pigs developed structural changes in the liver, characterized by a decrease in the number of cells in acini, an increase in the size of hepatocytes and their nuclei, an increase in the lumen of sinusoidal capillaries, which correlates with electrophoretic analysis - in the liver tissues of convalescent pigs in the region of less than 20 kDa there was an increase in the intensity of protein staining, which may include compounds differentially expressed in liver damage - inhibitors of metalloproteinases (28-18 kDa), peroxiredoxin (25-16 kDa), retinol-binding protein (20 kDa), haptoglobin alpha 2 chain (17 kDa) [10-13]. The detected damage to the liver tissue may be a consequence of hemorrhagic transformation [14] as a result of parenchymal hemorrhage [15] and indicate the limitation of the use of the liver of pigs recovered from intracerebral hematoma in the production of dietary-therapeutic products.

Acknowledgments. The authors are grateful to the Russian Science Foundation for funding this research with grant number 19-76-10034.

References

1. I. Chernukha, M. Nikitina, Potr. S. J. F. Sci. **14**, 264-270 (2020) <https://doi.org/10.5219/1312>
2. I. M. Chernukha, L. V. Fedulova, E. A. Kotenkova, S. Takeda, R. Sakata. Anim. Sci. J., **89**(5), 784-793 (2018) <https://doi.org/10.1111/asj.12986>
3. I. Chernukha, E. Kotenkova, S. Derbeneva, D. Khvostov, Int. J. Environ. Res. Public Health, **18**(14), 7330 (2021) <https://doi.org/10.3390/ijerph18147330>
4. I. Chernukha, L. Fedulova, E. Vasilevskaya, A. Kulikovskii, N. Kupaeva, E. Kotenkova, Saudi. J. Biol. Sci., **28**(5), 2877-2885 (2021) <https://doi.org/10.1016/j.sjbs.2021.02.020>
5. J. Burtscher, G.P. Millet, N. Place, B. Kayser, N. Zanou, Int. J. Mol. Sci. **22**(12), 6479 (2021) <https://doi.org/10.3390/ijms22126479>
6. A.G. Akhremko, M.A. Aryuzina, Vsyo o myase, **5S**, 46-48 (2020) <https://doi.org/10.21323/2071-2499-2020-5S-46-48>
7. I.M. Chernukha, L.V. Fedulova, A.G. Akhremko, E.A. Kotenkova, Potr. S. J. F. Sci., **11**(1), 398–402 (2017) <https://doi.org/10.5219/769>
8. N.L. Vostrikova, A.V. Kulikovskii, I.M. Chernukha, L.I. Kovalev, S.A. Savchuk, J. Anal. Chem. **72**(10), 1102-1112, (2017) <http://dx.doi.org/10.1134/S1061934817100173>
9. H.A. Alturkistani, F.M. Tashkandi, Z.M. Mohammedsaleh, Glob. J. Health Sci.; **8**(3), 72-79 (2015) <https://doi.org/10.5539/gjhs.v8n3p72>
10. C.L. Schoch, S. Ciuffo, M. Domrachev, C.L. Hotton, S. Kannan, R. Khovanskaya, D. Leipe, R. Mcveigh, K. O'Neill, B. Robbertse, S. Sharma, V. Soussov, J.P. Sullivan, L. Sun, S. Turner, I. Karsch-Mizrachi, *NCBI Taxonomy: a comprehensive update on curation, resources and tools. Database (Oxford)*, baaa062, (2020) <https://doi.org/10.1093/database/baaa062>
11. K.S. Nallagangula, K.N. Shashidhar, V. Lakshmaiah, C. Muninarayana. J. Circ. Biomark., **7**, 1849454418777186 (2018) <https://doi.org/10.1177/1849454418777186>
12. M.L. Chang, S.S. Yang, Cells, **8**(11), 1423 (2019) <https://doi.org/10.3390/cells8111423>
13. I.L. Karpenko, V.T. Valuev-Elliston, O.N. Ivanova, O.A. Smirnova, A.V. Ivanov, Antioxidants. **10**(6), 977 (2021) <https://doi.org/10.3390/antiox10060977>
14. A. Muscari, L. Faccioli, M.V. Lega, A. Lorusso, M. Masetti, M. P. Trossello, G.M. Puddu, L. Spinardi, M. Zoli, Brain Behav., **10**(1), e01497 (2020) <https://doi.org/10.1002/brb3.1497>
15. D. Veyel, K. Wenger, A. Broermann, T. Bretschneider, A.H. Luippold, B. Krawczyk, W. Rist, E. Simon, Sci. Rep., **10**, 1314 (2020) <https://doi.org/10.1038/s41598-020-58030-6>